Fluorescent cyclic peptides for cell imaging

Received: 25 April 2020 | Revised: 11 June 2020 | Accepted: 15 June 2020

DOI: 10.1002/pep2.24181

REVIEW

PeptideScience WILEY

Fluorescent cyclic peptides for cell imaging

Lorena Mendive-Tapia | Jinling Wang | Marc Vendrell

Centre for Inflammation Research, The University of Edinburgh, Edinburgh, UK

Correspondence
Lorena Mendive-Tapia and Marc Vendrell, Centre for Inflammation Research, The University of Edinburgh, Edinburgh EH16 4TJ, UK.
Email: l.mendive@ed.ac.uk (L. M.-T.) and marc.vendrell@ed.ac.uk (M. V.)

Funding information
ERC Consolidator, Grant/Award Number: 771443

Abstract

Fluorescent cyclic peptides are excellent chemical scaffolds to build optical agents for molecular imaging. In addition to their favorable physicochemical properties, they can be modified with multiple organic fluorophores and generate useful probes for biological assays targeting specific proteins, namely receptors or enzymes. In this article, we review recent advances in the synthetic approaches for the preparation of fluorescent cyclic peptides as well as some of their applications in biological imaging, from *in vitro* live-cell imaging studies to *in vivo* characterization of preclinical models.

KEYWORDS

amino acids, cancer, fluorescence, inflammation, probes

1 | INTRODUCTION

Peptides have been increasingly employed as chemical scaffolds to build molecular imaging agents. Peptide structures can form highly specific interactions with their respective biological targets, and therefore meet one of the main requirements in the design of imaging probes, that is, high specificity.[1] However, linear peptides exhibit some limitations that can hinder their application in biological studies. Their lability to proteolytic enzymes—particularly in diseased tissue where proteases may be abundant—has prompted the development of alternative chemical structures that can retain the molecular recognition properties of the peptides while displaying enhanced chemical stability.[2,3] Some of these alternative designs include the incorporation of unnatural amino acids, such as functionalised or D-amino acids,[4–8] into the peptide sequence as well as the cyclisation of linear peptides. Cyclic peptides are ubiquitously found in natural products, from complex macrocycles to small cyclodipeptides. The latter have been described as extremely compact and stable entities, which can form noncovalent self-assemblies to yield highly rigid biomimetic materials for diverse biotechnological and biomedical applications.[9] In this review, we will focus on cyclic peptides as frameworks to generate useful fluorescent probes for biological imaging studies.

Most peptides, including cyclic peptides, do not contain chemical groups that enable their detection by conventional techniques used in the biology labs, such as fluorimetric assays, fluorescence microscopy, or flow cytometry.[10] As a result, organic fluorophores have been incorporated into the peptide sequences to produce detectable contrast between the target cells and their surrounding microenvironment.[11] Furthermore, fluorescent cyclic peptides can be applied to many different biological experiments, from live-cell imaging to *in vivo* detection of cancer cells. Herein we review the advances in the synthetic approaches and applications of fluorescent cyclic peptides in biological imaging over the last 10 years. The review article is structured into two main sections. In the first one, we review different cyclopeptide topologies and synthetic chemical approaches for their labeling with small-molecule fluorophores. In the second one, we cover different examples of biological applications for fluorescent cyclic peptides, from *in vitro* studies focused on receptor expression or enzyme activity, to *in vivo* experiments in preclinical cancer models.

This article is dedicated to the memory of Prof. Nick Read for his contributions to the use of fluorescent peptides in biological imaging.

2 | CHEMICAL SYNTHESIS OF FLUORESCENT CYCLIC PEPTIDES

2.1 | Synthetic approaches for fluorescent peptide labeling

Natural aromatic amino acids such as tryptophan, tyrosine and phenylalanine exhibit intrinsic fluorescence in the ultraviolet range (λ_{exc}: 257-280 nm, λ_{em}: 282-350 nm)[12] and have been successfully employed in the development of green fluorescent protein (GFP) mutant variants or fusion tag structures for fluorescence protein labeling.[13,14] Nonetheless, their limited optical properties (e.g., short excitation and emission wavelengths, low brightness and photostability) have hampered their extensive use as biological dyes. Most commonly, the generation of fluorescent cyclic peptides for bioimaging relies on the chemoselective incorporation of an external fluorophore with suitable spectral properties into an appropriate position within a bioactive peptide. Careful attention of such parameters during probe

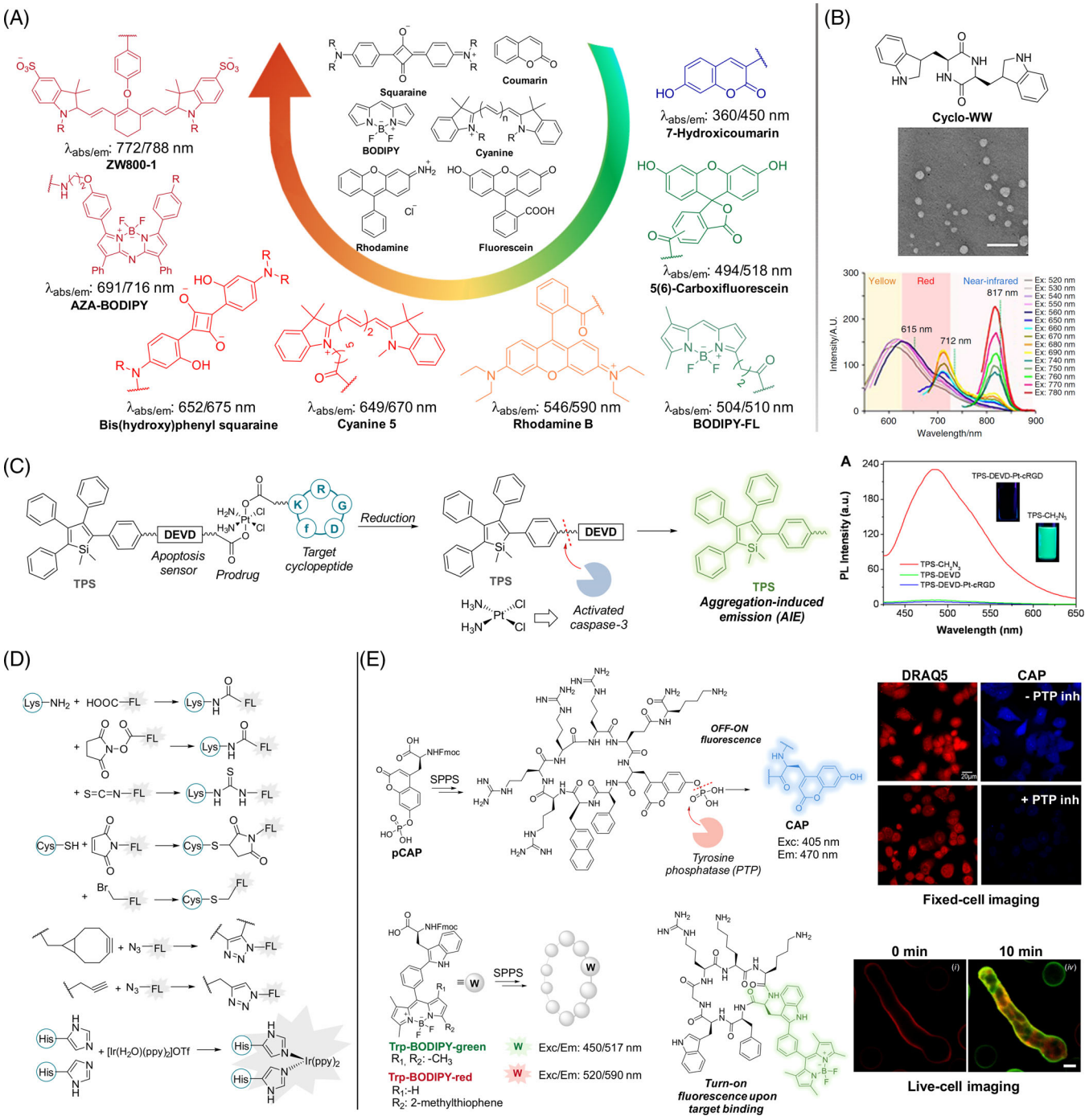

FIGURE 1 Legend on next page.

design is crucial to afford the desired bioimaging performance. At present, significant advances on synthetic chemistry have given rise to a diverse array of fluorophore options, many of them commercially available (Figure 1A). Dyes based on fluorescein, rhodamine, cyanine, and boron dipyrromethene (BODIPY) organic molecules are among the most popular fluorescent labels to date aimed to decipher a plethora of functions in biological systems.[15–21] Despite currently available options, new fluorophores with longer emission wavelengths and lower background fluorescence are in pressing need. Indeed, numerous efforts have been made to progress in the development of new near-infrared (NIR) fluorescent probes, particularly those with emission peaks appearing in the spectral range of the silent optical window (650-900 nm),[22] due to their deep penetration capabilities which can overcome photon attenuation in living tissue.[23] In addition to the traditionally explored squaraine and cyanine dyes, recent directions of new NIR fluorophores have pointed out the extension of the aromatic core of BODIPY or rhodamine scaffolds due to their excellent fluorescence quantum yields and photostability. Particularly, the hydrophilicity of rhodamine owing to its cationic character is considered an attractive feature for biological applications. Nonetheless, the exploration of further generations of these dyes is still an attractive and emerging topic of research.[24] The self-assembling of minimal cyclic peptide structures has also been implemented for the preparation of NIR nano-cluster chromophores with potential use in biological systems (Figure 1B).[25]

Over the past few decades, new approaches to improve the signal-to-noise ratios have been described. Activatable fluorophores, which are able to turn-on their fluorescence according to the characteristics of their surrounding environment, have attracted the attention of different disciplines because of their improved capabilities for imaging and wash-free features.[26–31] To achieve these fluorogenic properties, different sensing mechanisms have been successfully exploited, including aggregation-induced emission (AIE), photoinduced electron transfer (PeT), fluorescence resonance energy transfer (FRET), intramolecular charge transfer (ICT), and spirocyclisation. As an example, Liu, Tang and coworkers reported a theranostic probe for simultaneous drug delivery in cancer cells and in situ evaluation of its therapeutic killing response (Figure 1C).[32] The probe was composed of a platinum (IV) prodrug linked to a tetraphenylsilole (TPS) fluorophore with AIE sensing capabilities, a caspase-3 specific peptidyl apoptosis sensor and a cyclic peptide for targeting cancerous cells. On this system, only after activation of caspase-3 enzymes, the TPS fluorophore was cleaved from the apoptosis-sensing peptide sequence, triggering the AIE effect of the fluorophore and, therefore, turning the fluorescence on. Similarly, AIE-based phenomena has also been applied on minimal cyclic peptides for the detection of phenolic drugs.[33] Some PeT-dependent BODIPY fluorophore systems have been found to be sensitive to the polarity environment, showing increased fluorescence quenching in different microenvironments or upon binding to various analytes.[34–39]

Depending on the anchoring functional groups, the incorporation of the fluorescent moiety into the cyclic peptide is performed either before or after the cyclisation step through different covalent linkages such as amide,[40–42] thioamide,[43] and thioether[44] bonds, the former being the most widely applied (Figure 1D).[45] Additionally, numerous attempts have been made to explore alternative approaches.[46] When the coupling of the fluorophore takes place prior the cyclisation step, the amino or carboxylic acid terminal positions of the linear peptides are the preferred reactive points. For instance, Tamamura *et al*. reported a cyclic peptide inhibitor of the epidermal growth factor receptor (EGFR) evolved from the disulfide bond ring closure between two Cys residues and fluorescently labeled with fluorescein at the N-terminus through an amide bond linkage.[47] Nonetheless, most commonly the peptide ring closure involves both the α-amino and acid terminal functional groups. Therefore, the fluorophore is generally coupled after the cyclisation step to nucleophilic groups placed on the side chains of the peptide sequence, such as Cys (thiol), Ser (hydroxy), and Lys (amino), being the latter the most popular choice among

FIGURE 1 Common fluorophores and strategies for fluorescent peptide labeling. A, Representative selection of fluorescent cores (black and white) and reported fluorophores (colored) for the preparation of fluorescent cyclic peptides covering the blue to NIR fluorescent range. B, NIR nano-cluster chromophores evolved from the peptide self-assembling of tryptophan-tryptophan cyclic dipeptides (cyclo-WW) and Zn(II). Chemical Structure of cyclo-WW (top). Transmission electron microscopy image of the cyclo-WW + Zn(II) spherical nanospheres (middle) Scale bar: 300 nm. Emission spectra of the nanospheres in DMSO in a range of different excitation wavelengths (bottom). C, Mechanism of action of the multifunctional theranostic probe TPS-DEVD-Pt-cRGD for the in situ early evaluation of cisplatin drug effect in cancer cells by aggregation-induce fluorescence emission (left). Photoluminescence (PL) spectra of TPS-CH_2N_3, apoptosis sensor TPS-DEVD and TPS-DEVD-Pt-cRGD in DMSO/PIPES (v/v = 1/199) (right). Inset: corresponding pictures taken under irradiation of a UV lamp at 365 nm. D, Common amino acid side-chain coupling reactions for the chemical incorporation of fluorophores (FL) into cyclic peptides. E, Application of pCAP in SPPS for the preparation of the cell permeable c[(pCAP)FΦRRRRQ] peptide to detect intracellular tyrosine phosphatase (PTP) activity. Fixed-cell confocal microscopy images of MCF-7 human breast cancer cells treated with the labeled peptide (5 μM, blue fluorescence) and the nuclear stain DRAQ5 (red fluorescence) with and without pre-treatment with 1 mM sodium pervanadate as a PTP inhibitor (top). Trp-BODIPY amino acids with green and red fluorescent emission applied for the preparation of fluorescent cyclic peptides on SPPS. Representative example of c[RKKW(BODIPY) FWG] peptide with green fluorescent emission upon selective binding with *Aspergillus Fumigatus* fungal cells. Time-lapse high-resolution imaging of *A. fumigatus* upon incubation with a cell membrane counterstain (red) and the peptide (2 mM, green) for 0 and 10 minutes, respectively. Scale bar, 2.5 mm. (bottom). All images in part B were reproduced with permission from reference 25, Springer Nature Limited [publisher of ref. 25], the image in part C was reprinted (adapted) with permission from (Y. Yuan, R. T. K. Kwok, B. Z. Tang, B. Liu, *J. Am. Chem. Soc*. **2014**, *136*, 2546-2554), copyright (2014) American Chemical Society and all images in part E were reprinted (adapted) with permission from (Z. Qian, T. Liu, Y. Y. Liu, R. Briesewitz, A. M. Barrios, S. M. Jhiang, D. Pei. *ACS Chem. Biol*. **2013**; *8*, 423-431), copyright (2013) American Chemical Society and reference 54, Springer Nature Limited [publisher of reference 54]

all.[48,49] If required, the fluorophore conjugation is also extended with an additional linker spacer (e.g., PEG) to prevent steric hindrance interference of the fluorophore with peptide target recognition or to modulate chemical properties such as probe solubility. Lin, Yong and coworkers reported the incorporation of a 800CW cyanine dye to a peptide targeting tumor angiogenesis using a PEG spacer to improve the long-term circulation of the probe.[50]

An emerging alternative strategy of fluorescence peptide labeling relies on the direct preparation of non-natural fluorescent amino acid derivatives as building blocks for standard solid-phase peptide synthesis (SPPS).[10] This method affords great flexibility as it enables the selective incorporation of dyes anywhere in the peptide sequence using conventional SPPS procedures[51] and without the need of orthogonal side-chain protecting groups. On this basis, Pei and *et al*. reported a cell permeable peptide for detecting intracellular tyrosine phosphatase activities by embedding of a non-fluorescent phosphocoumaryl aminopropionic acid (pCAP), which behaves as a phosphotyrosine analogue, so that selective dephosphorylation by protein tyrosine phosphatases released the coumarin fluorescence (Figure 1E).[52] Recently, our group designed novel fluorescent Trp-BODIPY amino acids with green and red fluorescent emission that exhibit a fluorogenic behavior upon selective peptide target binding and also retain the lipophilic character of the native tryptophan, avoiding the modification of polar groups (e.g., amines and thiols) that may me crucial for the biological properties of the peptide (Figure 1E). These versatile amino acids have been successfully applied for the preparation of fluorescent cyclic peptides to image different processes associated with fungal infections and cancer.[53–56]

2.2 | Different fluorescent cyclopeptide topologies

In comparison to their linear counterparts, cyclic peptides possess reduced conformational freedom, which can result in improved biological properties. Constrained structures exhibit more resistance to chemical or enzymatic hydrolysis, better cell permeability and bind to their molecular targets with higher affinity and selectivity, enhancing their potential as therapeutics and biochemical research tools.[57,58] The synthetic preparation of cyclic peptides (typically around 5-14-mer) either mimicking natural structures or displaying novel archetypes is achieved through diverse approaches including phage display technology, split-intein circuit ligation, mRNA display, combinatorial chemistry as well as de novo synthesis. Thanks to their oligomeric nature based on sequential amino acid units conforming the amide bond backbone skeleton, automated SPPS approaches can be easily implemented. A representative example of a natural-mimicking cyclopeptide used for bioimaging purposes is octreotide, a somatostatin-like peptide which has been fluorescently labeled with fluorescein isothiocyanate for potential clinical usage in cancer diagnosis.[59] In another example, GX1, a cyclic 9-mer peptide identified by phage display technology, was labeled with a cyanine dye for fluorescence imaging of tumor vasculature.[60] According to the positions involved, peptide ring closure can be formed between the N-terminal and the C-terminal end, between side chains to either terminus or in between side chains through amide (homodetic) or other chemically stable bonds (heterodetic), such as disulphide bridges or ether, lactone and thioether linkages. Besides, other more complex cyclic topologies have also been produced thanks to the development of new chemical cross linker strategies in addition to traditional disulfide bond linkages between two Cys residues. In an example, a BODIPY-based fluorophore was conjugated to the C-terminal position of a stapled peptide evolved from the direct linkage of phenyl and tryptophan residues through a palladium-catalyzed CH activation reaction.[61] Alternative approaches involve the generation of cyclopeptide adducts whose fluorescence is encoded in the peptide sequence. An illustrative example was shown by Perrin *et al*., who prepared bicyclic fluorescent peptides via the condensation of an ortho-phthalaldehyde unit with the amine and thiol reactive groups of a cyclic peptide precursor to yield a fluorescent isoindole staple.[62] Other examples include the coordination of an iridium complex to the imidazole groups of histidine side chains of an RGD-containing peptide for simultaneous cyclisation and luminescence formation[63] and a double "click" cyclisation reaction from two biscyclooctynylated units of a linear precursor to yield cyclopeptide adducts bearing a bisazide fluorogenic dye.[64] Despite the simplicity of inherent fluorescent cyclic peptides, they often show suboptimal characteristics (e.g., wavelengths, quantum yields) for widespread application in molecular imaging.

Among all the cyclic peptide sequences described for the development of molecular imaging agents, special mention should be made to the Arg-Gly-Asp (RGD) tumor-homing motif for being one of the most prominent structures (Figure 2). The RGD motif has a long history of being used in the targeting of integrin transmembrane receptors, including α5β1, α8β1, αvβ1, αvβ3, αvβ5, αvβ6, αvβ8, and αIIbβ3 subtypes. Among all these, αvβ3 integrin, with an important role in the early phase of tumor forming and metastasis and overexpressed in several types of cancer, is currently the most widely studied.[65] RGD-containing cyclopeptides for αvβ3 integrin are predominantly based on the -RGDfV-,[66] -RGDyK-,[67] and -RGDfK-[42,68] sequences to afford improved target affinities, although other motifs have also been explored. For instance, the iRGD motif, whose cyclisation results from a disulfide bond between two Cys side chains groups, shows more efficient tumor penetration[69] and better cell internalization[70] for improved therapeutic performance. Chen *et al*. reported a NIR fluorescent iRGD-based peptide with affinity for αvβ3 integrin receptor with higher cellular staining for tumor-targeted imaging.[44] In another example, a dual-cargo iRGD peptide bearing two fluorescent dyes on each terminus was synthesized by Kim and coworkers to separately track the endocytic internalization and delivery of different fragments in cancer cells. In comparison to a control peptide having a non-iRGD sequence, such probe displayed better tumor imaging contrast.[71] More recently, efforts have been devoted to design RGD cyclopeptides to selectively image other relatively unexplored integrin receptors, such as αvβ8, with promising results.[72]

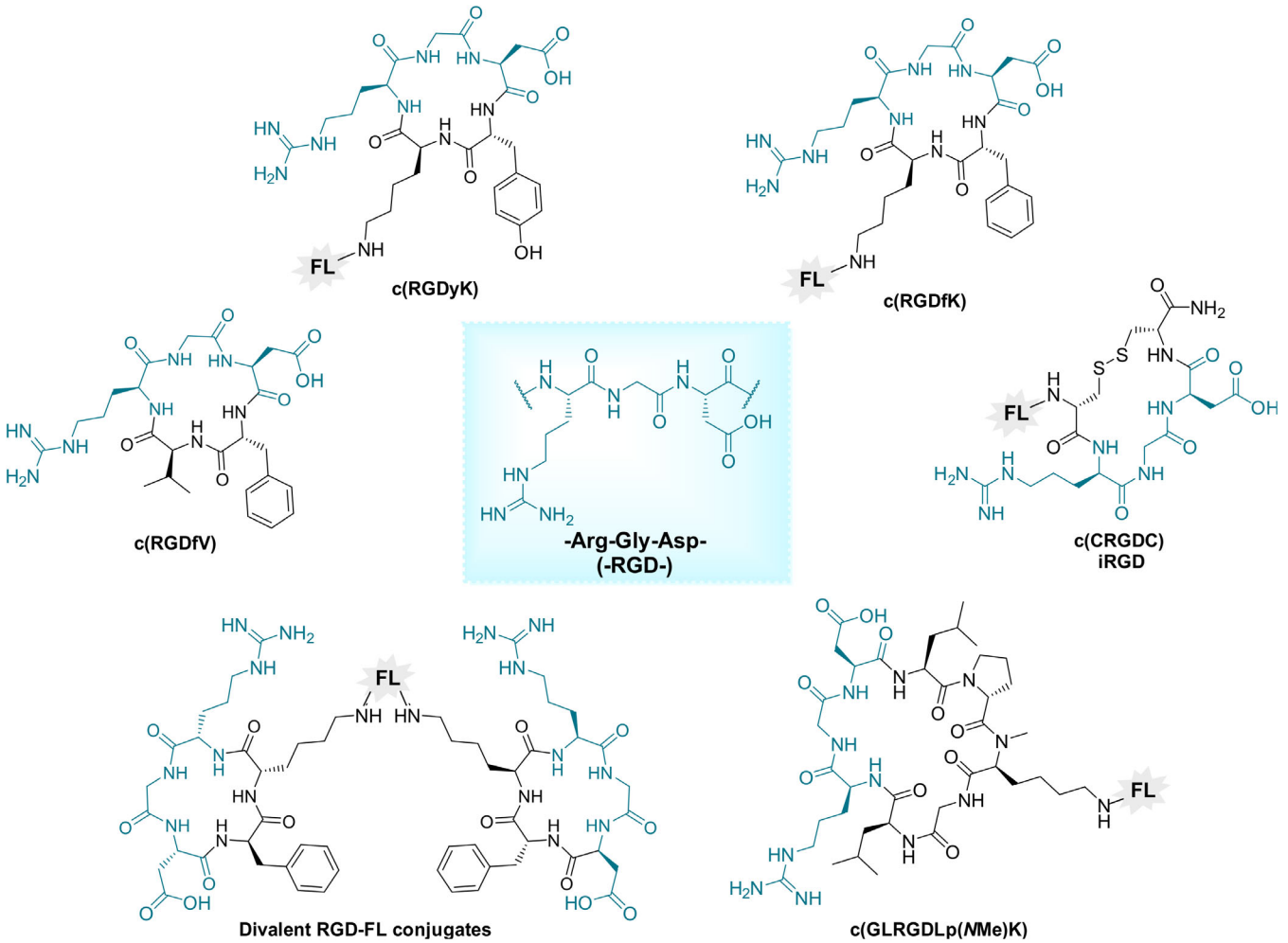

FIGURE 2 RGD-containing fluorescent cyclic peptide structures. Representative selection of peptide sequences including RGD motif: c(RGDyK), c(RGDfK), and c(RGDfV) peptides selective for αvβ3 integrin receptor, disulfide-based c(CRGDC) peptides named iRGD and divalent fluorescent RGD conjugates for improved tumor-targeted imaging, and c[GLRGDLp(*N*Me)K] peptide for selective imaging of αvβ8 integrin receptor. FL, fluorophore

The advancement on the development of new RGD probes have also given rise to the generation of novel systems. Smith and coworkers prepared a noncovalent probe by coupling a squaraine dye within a tetralactam macrocycle embedding a c(RGDfK) cancer targeting peptide.[73] This system exhibited remarkable high photostability and low phototoxicity for the fluorescent NIR detection of tumor cells *in vivo*. Further examples include a highly branched nanoprobe architecture evolved from the conjugation of c(RGDfK) peptide and a NIR cyanine dye onto polyamidoamine dendrimers for the identification of early stage esophageal squamous cell carcinoma and with potential theranostic applications.[74] Achilefu *et al*. reported the coupling of a NIR carbocyanine fluorophore to two units of c(RGDfK) peptide through their respective lysine side chains.[75] This approach achieved remarkable improvement in $\alpha_v\beta_3/\alpha_v\beta_5$ integrin binding affinity and tumor uptake compared to monovalent precursors. Similarly, Liu *et al*. reported a fluorescent probe bearing two cRGD moieties connected through different linkers to afford higher stability and faster binding kinetics for such receptors.[76]

3 | BIOLOGICAL APPLICATIONS OF FLUORESCENT CYCLIC PEPTIDE PROBES

As partially described in the section above, fluorescent cyclic peptides have been described for multiple applications in biological studies, from *in vitro* cell-based assays to *in vivo* imaging studies. Furthermore, their molecular versatility has facilitated their use for targeting different proteins, from cell-surface receptors to active enzymes or intracellular proteins. In this section, we will review some of the reported applications of fluorescent cyclic peptides for biological studies.

Many of the reports considering fluorescent cyclic peptides are focused on targeting biological receptors that are over-expressed in tumor tissues. As an example, Lu, Chen and coworkers developed Cy5.5-LyP-1, a tumor lymphatic-specific peptide including the fluorescent dye Cy5.5 to visualize lymphangiogenesis in tumor-draining lymph nodes.[77] This technology holds promise to detect high risk lymph nodes before tumor metastasis and after micro-metastasis. Furthermore, this peptide could accelerate the development of

antilymphatic therapeutics and improve our understanding of the interactions between cells in primary tumors and the tumor draining lymph nodes.

Other studies with fluorescent cyclic peptides have been focused on cell imaging by taking advantage of some differences (e.g., xenobiotic uptake) between diseased and healthy cells. The cyclic peptide analogue c(WXEAAYQkFL) was coupled to a carboxyfluorescein label through the amino group on the side chain of the D-lysine residue.[78] This new cyclic peptide proved to be preferentially uptaken by breast cancer cells and was used to detect them in human blood. Other conjugates using this peptide sequence include theranostic probes where the peptide was linked to chemotherapeutic drugs, such as doxorubicin, in order to increase their target efficacy.[79]

Fluorescent cyclic peptides can be also directed to specific compartments of the cell. Our group previously reported the fluorogenic Trp-BODIPY amino acid to prepare an environmentally-sensitive analogue of the antimicrobial cyclic peptide PAF26 with high affinity for the membranes of fungal cells.[54] In this case, the use of a fluorogenic label enabled to brightly stain the membranes of the fungal pathogen *Aspergillus fumigatus* with high signal-to-noise ratios and without the need for washing steps (Figure 1E). In another example, Trp-BODIPY amino acid was employed for the preparation of a fluorescent cyclic lactadherin mimic for the detection of apoptotic bodies[55] as well as a fluorescent cyclopeptide for the quantification of drug-induced apoptosis,[80] displaying strong binding in a Ca^{2+} independent-manner, unlike the gold standard for apoptosis detection Annexin V. Fluorophore-bearing oligomers of cyclic dipeptides have also been implemented for the intracellular delivery of pDNA.[81] Other peptides have been described to target intracellular organelles. On this basis, the rapid uptake and subcellular localization of fluorescently-labeled analogues of the cyclic depsipeptide kapakahine E was reported.[82] Specific localisation within the Golgi apparatus was confirmed by colocalization experiments with other commercially-available markers. Nucleic acids are another example of widely targeted macromolecules inside cells. Yavin and coworkers synthesized FITC-labeled peptide nucleic acids with a cyclic structure and confirmed their uptake in U87MG glioblastoma cells as well as their blocking function of miR-155, a reported oncogenic miRNA.[83]

Cyclic fluorescent peptides have also been developed to target liposomes. In the work reported by Dreher and coworkers, a novel cyclic peptide including the NGR motif (cKNGRE) was conjugated to the pH-sensitive Oregon Green dye.[84] These conjugates showed good affinity to the CD13 marker found in cancer cells, and were further used to favor the delivery of doxorubicin into tumors.

3.1 | Fluorescent cyclic peptides targeting cell receptors

As described before, cyclic peptides including the RGD structure can bind to integrin-type receptors with high affinity. Vahrmeijer *et al*. designed a fluorescent cyclic peptide including a cyclic RGD motif and label it with the NIR ZW800-1 dye for intraoperative imaging. The NIR peptide was found to bind multiple integrin receptors and therefore could be used to detect different types of cancer.[85] In an attempt to improve the cellular uptake performance, the group of Smith described the preparation of novel fluorescent probes including the squaraine fluorophore with deep red fluorescence emission. Squaraine dyes were conjugated to a collection of cyclic RGD-containing peptides with variable targeting properties in ovarian cancer cells and the divalent conjugate was found to exhibit the highest cellular uptake.[86] In another example, Tang, Liu and coworkers built up a cyclic RGD peptide with AIE characteristics and a caspase-activatable motif so that increased fluorescence was observed in regions with high caspase activity.[87,88]

Another important cell-surface receptor that has been targeted with fluorescent cyclic peptides is the hepatocyte growth factor receptor (HGFR), also called c-Met. This receptor is present on the surface of tumor cells in several types of cancer, such as gastric carcinoma,[89] ovarian cancer,[90] and colorectal polyps,[91] Among others. Using a randomized platform to produce non-natural macrocyclic peptides, Suga, Lee, and coworkers optimized a HGFR-binding macrocyclic peptide that was subsequently labeled with fluorescein. The peptide showed high c-Met binding affinity in gastric carcinoma cells and showed promising results for *in vivo* imaging.[89] Similarly, the Cy5-labeled cyclic peptide GE137 was reported by Burggraaf *et al*. as a molecular probe to detect HGFR in ovarian cancer cells (Figure 3A). The peptide sequence included two disulphide bonds between four cysteine residues, which were essential for high binding affinity to the receptor. The GE137 peptide displayed specific binding to c-Met in colorectal polyps, as well as good water solubility.[91]

Oxytocin receptors are another interesting group of proteins that have been widely studied. Like other hormones, oxytocin has important functions as chemical messengers and key roles in the reproductive system. To further study these receptors, Karpenko *et al*. reported the conjugation of a stable version of oxytocin, named carbetocin, to the environmentally-sensitive Nile Red dye using a PEG spacer and produced a turn-on fluorescent probe with improved capabilities for oxytocin imaging.[92] The related vasopressin-type receptors have been also subject of study because of their neuroendocrine effect as well as cognitive and behavioral functions, among others. In this context, the group of Manning reported the first peptide to detect the specific localisation of V1b-type vasopressin receptors in brain. The fluorescent cyclic peptide was based on the structure of vasopressin (d[Leu4, Lys8]VP)[93] and included one molecule of AlexaFluor 647 as the fluorophore.

Recently, our group disclosed the preparation of a red fluorescent analogue of a cyclopeptide with high affinity for keratin-1 (KRT1) cell receptor, overexpressed in aggressive breast cancer tumors, that enabled the simultaneous imaging of KRT1+ cancerous cells in combination with tumor-associated macrophage markers in tumor tissue samples (Figure 3B).[56] Finally, other peptides have been reported to target EGFR, which is central in multiple signaling pathways related to cell proliferation and differentiation. EGFR are often over-expressed in cancer cells and Tamamura *et al*. described a series of cyclic decapeptide analogues including a bright fluorescein moiety as functional inhibitors of the dimerization between the EGF monomers.[47]

3.2 | Fluorescent cyclic peptides targeting enzymes

Matrix metalloproteinases (MMPs) are enzymes with proteolytic activity against a broad range of extracellular matrix proteins. MMPs are involved in the cleavage of cell surface receptors as well as in the release of apoptotic ligands and activation of chemokines.[94] MMPs are essential enzymes and play important roles in multiple biological processes, such as proliferation, migration, adhesion, and differentiation among others. Gelatinases are a subgroup of MMPs that have

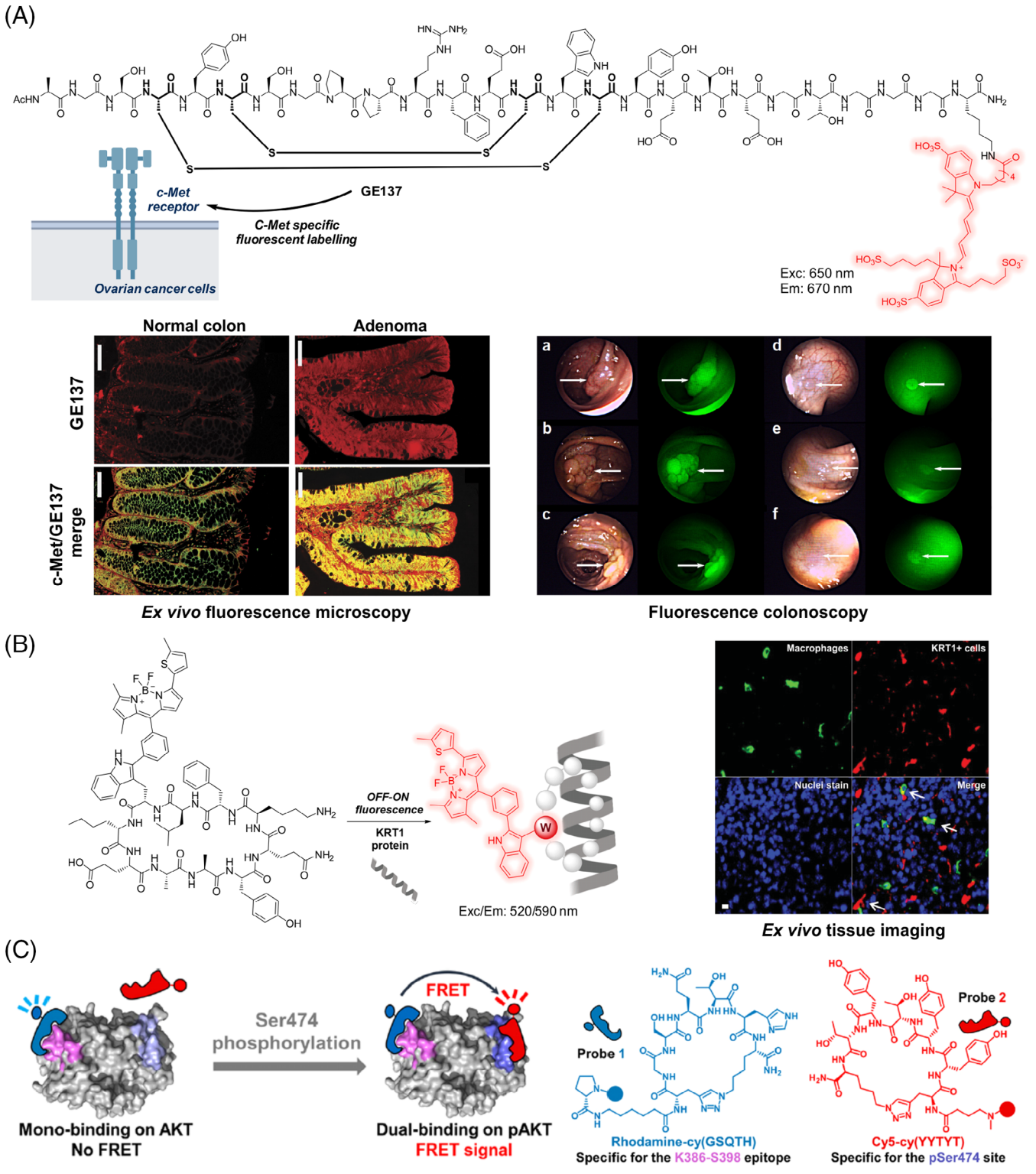

FIGURE 3 Legend on next page.

been described in tumor progression, angiogenesis, and metastasis.[95] Li and coworkers described fluorescent cyclic peptides bearing the HWGF motif and a fluorescent Cy5.5 reporter.[96] Notably, two different cyclisation strategies were pursued, and cyclic peptides were either formed by disulphide bonds or via intracellular amide linkages. The two different conjugates were compared for binding to the target, and the latter exhibited greater stability, providing an efficient probe to image gelatinases. Similarly, Jeong *et al*. designed a Cy5.5-labeled fluorescent cyclic peptide for imaging of the enzyme MMP-2, which was detected in colonic lesions of an inflammation-induced colorectal cancer model.[97] More recently, Xue *et al*. described a novel chemical method to analyze the intracellular activity of AKT.[98] AKT plays a crucial role in cell survival, being related to oncogenesis and tumor maintenance. The authors employed a FRET strategy to couple a pair of cyclic peptides targeting two different regions of the protein: (a) the phosphorylated site of Ser474 and (b) a distal epitope of AKT (Figure 3C). The resulting construct displayed a fluorescent signal contingent upon AKT phosphorylation and was used to profile the intracellular dynamics of AKT signaling.

3.3 | Fluorescent cyclic peptides targeting other biomolecules

The complexes between fibrin and fibronectin are abundant in the tumor microenvironment but they are rarely present in normal tissues. This feature makes them valuable targets for tumor imaging. In this context, Wang *et al*. described the cyclic peptide iCREKA for targeting and imaging the tumor stroma.[99] FITC-labeled iCREKA peptides displayed binding to fibrin-fibronectin complexes and subsequent permeabilisation into glioma cells.

In a related context, the extra domain B of fibronectin (EDB-FN) mediates cell adhesion and migration, and its expression is related to multiple processes in cancer. To specifically target EDB-FN in prostate cancer, Lu and coworkers designed a Cy5-labeled cyclic version of the ZD2 peptide (sequence: CTVRTSADC).[100] This peptide showed good capabilities for optical molecular imaging and potential applications for the diagnosis and treatment of prostate cancer. Alternative approaches for targeting proteins with NIR fluorescent peptides include the cyclic albumin-binding domain peptide conjugated for lymphatic imaging[101] or the histone H_1-binding peptide for imaging apoptosis *in vivo* as a response to anticancer treatments.[102]

Actin is one of the most abundant proteins in eukaryotic cells and is widely involved in cell division and cell signaling. On this basis, analogues of the natural cyclic peptides jasplakinolide and chondramide C, which behave as actin-stabilizing structures, have been rationally designed and optimized. These peptides have been modified with a green fluorescent BODIPY reporter and used for imaging static actin in fixed permeabilized as well as nonpermeabilised cells.[103] This study rendered nontoxic cyclic peptides as nontoxic and cell-permeable probes to selectively image static, long-lived actin filaments against dynamic F-actin and monomeric G-actin populations in live cells, with negligible disruption of rapid actin dynamics. More recently, Lukinavicius and coworkers have described rhodamine derivatives of jasplakinolide which are efflux-insensitive and enabled G- and F-actin structures in live cells.[104]

3.4 | *In vivo* imaging using fluorescent cyclic peptides

A major feature of fluorescence imaging is its capability to visualize biological systems at multiple levels, from microscopy images with subcellular resolution to whole-body images where probes found in different tissues within a living organism can be monitored simultaneously. *In vivo* imaging is advantageous in that it allows examination of a biological question in the native microenvironment and under physiological conditions. Many probes for *in vivo* imaging, particularly fluorophores emitting in the NIR region of the spectra,[105–109] have been described.

In the last 15 years, there has been a lot of interest to modulate the optical properties of fluorescent scaffolds[110–113] (e.g., excitation/emission, water solubility, fluorescence lifetime) to generate probes with improved characteristics for *in vivo* imaging. In addition to widely used commercial fluorophores, such as cyanines or rhodamines, fluorophores with additional features have been developed. Achilefu *et al*. reported a pH-sensitive construct composed of a pH-activatable cyanine dye and cyclic RGD peptide for targeting and

FIGURE 3 Examples of applications of fluorescent cyclic peptide probes. A, GE137 fluorescent peptide with selective targeting against c-Met receptor in ovarian cancer cells. ex vivo fluorescence microscopy images of tissue sections from normal colon and adenomatous polyp biopsies taken after GE137 administration (red fluorescence) and overlap (shown in yellow) with immunohistochemical staining for c-Met (bottom left). Simultaneous white and fluorescent colonoscopy images from patients, showing representative lesions with increased fluorescence (a-f, bottom right). Polyps are indicated by the white arrows. B, Fluorogenic Trp-BODIPY (red) cyclopeptide targeting Keratin 1 (KRT1) protein for imaging of aggressive carcinomas. ex vivo tissue imaging of aggressive carcinomas displaying multicolour staining of tumor-associated macrophages with anti-Iba1 (green), KRT1+ cells with peptide (red) and DAPI nuclear stain (blue) (right). macrophage-cancer cell interactions are identified with white arrows. Scale bar: 10 mm. C, Förster resonance energy transfer (FRET)-based phosphorylated AKT (pAKT) detection strategy for profiling intracellular AKT protein kinase activity based on the dual coupling of two probes: a rhodamine-cy(GSQTH) peptide targeting the K386-S398 epitope (probe 1, blue) and a cyanine5-cy(YYTYT) peptide targeting the phosphorylated site of Ser474 of AKT (probe 2, red). The resulting construct displayed the red fluorescent signal of probe 2 only upon AKT phosphorylation. All images in part A were reproduced with permission from ref. [91], Springer Nature Limited [publisher of ref. 91], the image in part B was reproduced with permission from ref. [56], published by The Royal Society of Chemistry, and all images in part C were reprinted (adapted) with permission from (S. Shao, Z. Li, H. Cheng, S. Wang, N. G. Perkins, P. Sarkar, W. Wei, M. Xue. *J Am Chem Soc*. **2018**; *140*, 13586-13 589), copyright (2018) American Chemical Society

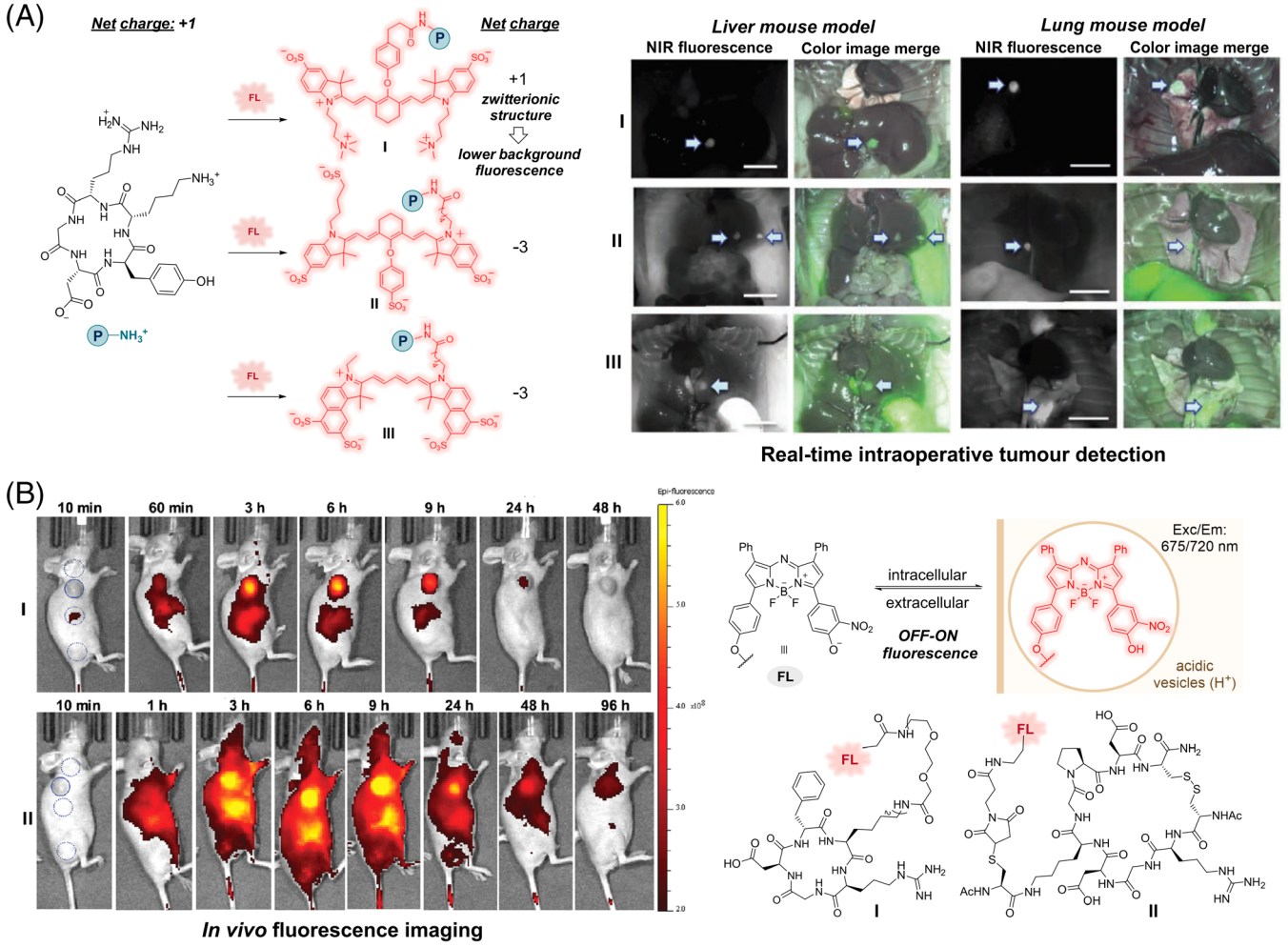

FIGURE 4 Examples of *in vivo* imaging applications with fluorescent cyclic peptide probes. A, Near-infrared fluorescent c(RGDyK)-based probes I to III for tumor imaging. Probe I displaying a zwitterionic structure maintains the net charge of the original c(RGDyK) molecule at physiological pH, avoiding disruption of local protein folding, nonspecific binding and lowering the background fluorescence. Real-time intraoperative liver (left) and lung (right) tumor detection using NIR-fluorescent probes I to III (10 nmol each) which were injected intravenously into each mouse 4 hours before imaging. Shown are representative (n = 5 mice per group) NIR fluorescence images and a pseudocoloured merge with color images. Open arrows indicate tumors. B, Activatable NIR-AZA fluorescent probes sensitive to intracellular acidic environments bearing c(RGDfK) (I) or c(CRGDKGPDC) (II) cyclopeptides. (right). *In vivo* fluorescence imaging of probes I (13.2 nmol, upper panel) and II (10.5 nmol, lower panel) in MDA-MB 231 human breast tumor models at different time points (left). First image of each panel shows selected tumor region of interest (ROI) (solid circle) and three background ROIs (dashed circles). Fluorescence remained silent within the vasculature until 60 minutes post injection, when probes began to accumulate at the tumor region. Color scale bar shows epifluorescence quantified in radiant efficiency units [(p/sec/cm^2/sr)/(μW/cm^2)], min = 2·10^8, max = 6·10^8. FL, fluorophore. All images in part A were reproduced with permission from ref. [115], Springer Nature Limited [publisher of ref. 115] and all images in part B were reproduced with permission from ref. [123], published by The Royal Society of Chemistry

imaging acidic tumor lysosomes in an orthotopic breast tumor mouse model.[114] The groups of Vahrmeijer and Frangioni reported zwitterionic NIR fluorophores which were incorporated into cRGD peptides for tumor imaging (Figure 4A).[85,115] These peptides were compatible with protocols used during surgery and showed potential for real-time imaging of cancer cells with low background fluorescent signals. In another approach, fluorescent magnetic nanoparticles were conjugated to the cyclic RGDyE peptide for hybrid magnetic resonance and optical *in vivo* imaging of human breast tumors, showing no acute toxicity.[116]

In addition to the use of sophisticated fluorophores, another strategy to improve the *in vivo* imaging performance of fluorescent cyclic peptides relies on the modification of the conjugated peptides, such as structures with dual targeting capabilities, minimal *in vivo* toxicity and enhanced biodistribution. For instance, Lou, Xia and coworkers designed a fluorescent construct composed of cNGR and cRGD peptides for dual targeting of CD13 aminopeptidase and integrin receptors, respectively.[117] In another example, Boturyn *et al.* designed a fluorescent probe containing the sequences cRGD and ATWLPPR, a peptide that behaves as a specific ligand for the

neuropilin-1 protein receptor which is over-expressed in the extracellular plasma membrane of tumor cells.[118] Notably, the authored compared the biological effects of injecting the dual fluorescent construct as well as the separate injection of the two peptide sequences and found a faster and more specific accumulation in tumors of the peptide conjugate, which was attributed to the stabilization of NRP1 at the cell membrane surface. Larger constructs have been also developed, such as poly(amidoamine) dendrimers, which were modified by incorporation of the NIR dye cypate and the iRGD peptide and used to visualize accumulation in tumors as a potential strategy to test delivery of anticancer drugs using dendrimers.[70]

Although the most common cyclic peptides for *in vivo* imaging of tumors are based on the RGD motif due to its high binding affinity for integrin receptors, some other cyclic peptides have shown interesting applications. For example, Ge and coworkers reported novel cyclic peptides bearing the RKD motif as proapoptotic ligands[119] of the glucose-regulated protein 78 kDa (GRP78) which is over-expressed on the cell surface of several types of cancer.[120] Similarly, and considering the high levels of endothelial growth factor receptors (EGFR) in colorectal cancer cells, Jois *et al.* reported a highly stable cyclic derivative based on the EGFR-specific peptide ligand LARLLT.[121] In another example, a cyclic peptide including the RPMC motif and a fluorescein reporter was described to specifically detect colon cancer cells by targeting integrin-type receptors.[122] This peptide was applied for real-time endoscopic tumor detection in an orthotopic colon mouse model, even when tumors were submucosal and with prolonged fluorescence signals after systemic injection.

Finally, one of the main translational applications of *in vivo* fluorescence imaging is its potential use for intraoperative imaging given the emerging interest in fluorescence-guided surgery to improve the identification of tumor margins and optimize the outcomes of tumor resection. In this context, O'Shea *et al.* recently reported a chemical approach to enhance the signal-to-noise ratios of fluorescent cyclic peptides by conjugating them to NIR activatable fluorophores that preferentially emit in acidic microenvironments (Figure 4B).[123] The authors prepared activatable constructs containing the acid-sensitive NIR-AZA fluorophore and iRGD or cRGD peptides. The peptides were tested *in vivo* in mouse models with subcutaneous tumors and showed higher signal-to-noise ratios to the cyclic peptides that were conjugated to always-on NIR fluorophores.

4 | CONCLUSIONS

The notable physicochemical and biological properties of cyclic peptides make them interesting scaffolds for the preparation of molecular imaging agents. Multiple approaches for the synthesis, characterization and validation of fluorescent cyclic peptides in biological systems have been reported and reviewed in this article. These strategies include the optimization of peptide constructs with unique biochemical features (e.g., improved permeability and proteolytic stability, stapled peptides, high binding affinity to specific receptors or enzymes) as well as the introduction of fluorescent labels with suitable optical properties (e.g., from fluorogenic amino acids that turn-on upon target recognition to bespoke NIR dyes). With a rapidly growing molecular toolbox and well-established synthetic methodologies in place, the applications for fluorescent cyclic peptides in biological studies will steadily increase over the coming years. Their proven compatibility with a broad range of imaging modalities (i.e., high-throughput screens, multiphoton microscopy, and intravital imaging) will enable their use in drug discovery programs for cell reprogramming[124,125] as well as in mechanistic studies to characterize cells in tissue microenvironments[126] and in clinical applications,[127] where novel and highly specific probes are required. We anticipate that fluorescent cyclic peptides will also facilitate the construction of dual probes with multimodal character, that is, compatible with different imaging modalities and also theranostic probes able to deliver imaging reporters as well as therapeutic loads. Their integration into current strategies for the preparation of activatable fluorescent prodrugs[106,128] or smart molecular imaging agents[129] will likely produce the next generation of smart probes able to address complex biological questions and to assist in the development of new therapies for personalized medicine.

ACKNOWLEDGEMENT

Marc Vendrell acknowledges funding from an ERC Consolidator Grant (771443).

CONFLICT OF INTEREST

The authors declare no conflict of interests.

ORCID

Marc Vendrell https://orcid.org/0000-0002-5392-9740

REFERENCES

[1] M. L. James, S. S. Gambhir, *Physiol. Rev.* **2012**, *92*, 897.
[2] M. Erak, K. Bellmann-Sickert, S. Els-Heindl, A. G. Beck-Sickinger, *Bioorg. Med. Chem.* **2018**, *26*, 2759.
[3] D. A. Guarracino, J. A. Riordan, G. M. Barreto, A. L. Oldfield, C. M. Kouba, D. Agrinsoni, *Chem. Rev.* **2019**, *119*, 9915.
[4] A. Molero, M. Vendrell, J. Bonaventura, J. Zachmann, L. López, L. Pardo, C. Lluis, A. Cortés, F. Albericio, V. Casadó, M. Royo, *Eur. J. Med. Chem.* **2015**, *97*, 173.
[5] M. Vendrell, A. Molero, S. Gonzalez, et al., *J. Med. Chem.* **2011**, *54*, 1080.
[6] A. Soriano, M. Vendrell, S. Gonzalez, J. Mallol, F. Albericio, M. Royo, C. Lluís, E. I. Canela, R. Franco, A. Cortés, V. Casadó, *J. Pharmacol. Exp. Ther.* **2010**, *332*, 876.
[7] M. Vendrell, A. Soriano, V. Casado, et al., *ChemMedChem* **2009**, *4*, 1514.
[8] M. Vendrell, E. Angulo, V. Casado, et al., *J. Med. Chem.* **2007**, *50*, 3062.
[9] S. Manchineella, T. Govindaraju, *ChemPlusChem* **2017**, *82*, 88.
[10] Z. Cheng, E. Kuru, A. Sachdeva, M. Vendrell, *Nat. Rev. Chem.* **2020**, *4*, 275.
[11] D. Schumacher, C. P. Hackenberger, *Curr. Opin. Chem. Biol.* **2014**, *22*, 62.
[12] F. W. J. Teale, G. Weber, *Biochem. J.* **1957**, *65*, 476.
[13] E.-M. Siepert, E. Gartz, M. K. Tur, H. Delbrück, S. Barth, J. Büchs, *BMC Biotechnol.* **2012**, *12*, 65.

[14] R. Y. Tsien, *Annu. Rev. Biochem.* **1998**, *67*, 509.
[15] T. Nagano, *Proc. Jpn. Acad. Ser. B.* **2010**, *86*, 837.
[16] C. Zhao, A. Fernandez, N. Avlonitis, G. Vande Velde, M. Bradley, N. D. Read, M. Vendrell, *ACS Comb. Sci.* **2016**, *18*, 689.
[17] G. G. Dias, A. King, F. de Moliner, M. Vendrell, E. N. da Silva Junior, *Chem. Soc. Rev.* **2018**, *47*, 12.
[18] T. B. Gontijo, R. P. de Freitas, F. S. Emery, L. F. Pedrosa, J. B. Vieira Neto, B. C. Cavalcanti, C. Pessoa, A. King, F. de Moliner, M. Vendrell, E. N. da Silva Júnior, *Bioorg. Med. Chem. Lett.* **2017**, *27*, 4446.
[19] J. S. Lee, M. Vendrell, Y. T. Chang, *Curr. Opin. Chem. Biol.* **2011**, *15*, 760.
[20] F. De Moliner, K. Knox, A. Reinders, et al., *J. Exp. Bot.* **2018**, *69*, 2473.
[21] M. Knoblauch, M. Vendrell, E. de Leau, A. Paterlini, K. Knox, T. Ross-Elliot, A. Reinders, S. A. Brockman, J. Ward, K. Oparka, *Plant Physiol.* **2015**, *167*, 1211.
[22] K. Umezawa, D. Citterio, K. Suzuki, *Anal. Sci.* **2014**, *30*, 327.
[23] J. Rao, A. Dragulescu-Andrasi, H. Yao, *Curr. Opin. Biotechnol.* **2007**, *18*, 17.
[24] D. Wu, S. Cheung, M. Devocelle, L. J. Zhang, Z. L. Chen, D. F. O'Shea, *Chem. Commun.* **2015**, *51*, 16667.
[25] K. Tao, Z. Fan, L. Sun, P. Makam, Z. Tian, M. Ruegsegger, S. Shaham-Niv, D. Hansford, R. Aizen, Z. Pan, S. Galster, J. Ma, F. Yuan, M. Si, S. Qu, M. Zhang, E. Gazit, J. Li, *Nat. Commun.* **2018**, *9*, 3217.
[26] B. M. Luby, D. M. Charron, C. M. Maclaughlin, G. Zheng, *Adv. Drug Deliv. Rev.* **2017**, *113*, 97.
[27] N. Kielland, M. Vendrell, R. Lavilla, Y. T. Chang, *Chem. Commun.* **2012**, *48*, 7401.
[28] F. de Moliner, N. Kielland, R. Lavilla, M. Vendrell, *Angew. Chem. Int. Ed.* **2017**, *56*, 3758.
[29] A. Vazquez-Romero, N. Kielland, M. J. Arevalo, et al., *J. Am. Chem. Soc.* **2013**, *135*, 16018.
[30] O. Ghashghaei, S. Caputo, M. Sintes, M. Revés, N. Kielland, C. Estarellas, F. J. Luque, A. Aviñó, R. Eritja, A. Serna-Gallego, J. A. Marrugal-Lorenzo, J. Pachón, J. Sánchez-Céspedes, R. Treadwell, F. de Moliner, M. Vendrell, R. Lavilla, *Chemistry* **2018**, *24*, 14513.
[31] R. Treadwell, F. de Moliner, R. Subiros-Funosas, T. Hurd, K. Knox, M. Vendrell, *Org. Biomol. Chem.* **2018**, *16*, 239.
[32] Y. Yuan, R. T. K. Kwok, B. Z. Tang, B. Liu, *J. Am. Chem. Soc.* **2014**, *136*, 2546.
[33] C. Balachandra, T. Govindaraju, *J. Org. Chem.* **2020**, *85*, 1525.
[34] H. Sunahara, Y. Urano, H. Kojima, T. Nagano, *J. Am. Chem. Soc.* **2007**, *129*, 5597.
[35] M. Sintes, F. De Moliner, D. Caballero-Lima, et al., *Bioconjug. Chem.* **2016**, *27*, 1430.
[36] M. Virelli, W. Wang, R. Kuniyil, J. Wu, G. Zanoni, A. Fernandez, J. Scott, M. Vendrell, L. Ackermann, *Chemistry* **2019**, *25*, 12712.
[37] L. Zhang, J. C. Er, H. Jiang, X. Li, Z. Luo, T. Ramezani, Y. Feng, M. K. Tang, Y. T. Chang, M. Vendrell, *Chem. Commun.* **2016**, *52*, 9093.
[38] M. Vendrell, G. G. Krishna, K. K. Ghosh, D. Zhai, J. S. Lee, Q. Zhu, Y. H. Yau, S. G. Shochat, H. Kim, J. Chung, Y. T. Chang, *Chem. Commun.* **2011**, *47*, 8424.
[39] D. Zhai, S. C. Lee, M. Vendrell, L. P. Leong, Y. T. Chang, *ACS Comb. Sci.* **2012**, *14*, 81.
[40] M. Nahrwold, C. Weiss, T. Bogner, et al., *J. Med. Chem.* **2013**, *56*, 1853.
[41] A. Sajid, N. Raju, S. Lusvarghi, S. Vahedi, R. E. Swenson, S. V. Ambudkar, *Drug Metab. Dispos.* **2019**, *47*, 1013.
[42] Z. Hu, R. L. Arrowsmith, J. A. Tyson, V. Mirabello, H. Ge, I. M. Eggleston, S. W. Botchway, G. Dan Pantos, S. I. Pascu, *Chem. Commun.* **2015**, *51*, 6901.
[43] P. Di Pietro, L. Zaccaro, D. Comegna, et al., *RSC Adv.* **2016**, *6*, 112381.
[44] Y. Ye, L. Zhu, Y. Ma, G. Niu, X. Chen, *Bioorg. Med. Chem. Lett.* **2011**, *21*, 1146.
[45] C. Zhao, L. Mendive-Tapia, M. Vendrell, *Arch. Biochem. Biophys.* **2019**, *661*, 187.
[46] K. A. Jolliffe, *Acc. Chem. Res.* **2017**, *50*, 2254.
[47] K. Toyama, T. Mizuguchi, W. Nomura, H. Tamamura, *Bioorg. Med. Chem.* **2016**, *24*, 3406.
[48] M. H. Lee, J. Y. Kim, J. H. Han, S. Bhuniya, J. L. Sessler, C. Kang, J. S. Kim, *J. Am. Chem. Soc.* **2012**, *134*, 12668.
[49] R. J. Brea, M. E. Vázquez, M. Mosquera, L. Castedo, J. R. Granja, *J. Am. Chem. Soc.* **2007**, *129*, 1653.
[50] L. Liu, G. Lin, F. Yin, W. C. Law, K. T. Yong, *J. Biomed. Mater. Res. Part A.* **2016**, *104A*, 910.
[51] F. Yraola, R. Ventura, M. Vendrell, A. Colombo, J. C. Fernàndez, N. de la Figuera, D. Fernández-Forner, M. Royo, P. Forns, F. Albericio, *QSAR Comb. Sci.* **2004**, *23*, 145.
[52] Z. Qian, T. Liu, Y. Y. Liu, R. Briesewitz, A. M. Barrios, S. M. Jhiang, D. Pei, *ACS Chem. Biol.* **2013**, *8*, 423.
[53] L. Mendive-Tapia, R. Subiros-Funosas, C. Zhao, F. Albericio, N. D. Read, R. Lavilla, M. Vendrell, *Nat. Protoc.* **2017**, *12*, 1588.
[54] L. Mendive-Tapia, C. Zhao, A. R. Akram, S. Preciado, F. Albericio, M. Lee, A. Serrels, N. Kielland, N. D. Read, R. Lavilla, M. Vendrell, *Nat. Commun.* **2016**, *7*, 10940.
[55] R. Subiros-Funosas, L. Mendive-Tapia, J. Sot, J. D. Pound, N. Barth, Y. Varela, F. M. Goñi, M. Paterson, C. D. Gregory, F. Albericio, I. Dransfield, R. Lavilla, M. Vendrell, *Chem. Commun.* **2017**, *53*, 945.
[56] R. Subiros-Funosas, V. C. L. Ho, N. D. Barth, L. Mendive-Tapia, M. Pappalardo, X. Barril, R. Ma, C. B. Zhang, B. Z. Qian, M. Sintes, O. Ghashghaei, R. Lavilla, M. Vendrell, *Chem. Sci.* **2020**, *11*, 1368.
[57] J. S. Choi, S. H. Joo, *Biomol. Ther.* **2020**, *28*, 18.
[58] X. Jing, K. Jin, *Med. Res. Rev.* **2020**, *40*, 753.
[59] F. Bianying, G. Linjie, W. Lihua, L. Fan, L. Jianxin, G. Jimin, F. Chunhai, H. Qing, *Anal. Chem.* **2013**, *85*, 7732.
[60] K. Chen, L. P. Yap, R. Park, X. Hui, K. Wu, D. Fan, X. Chen, P. S. Conti, *Amino Acids* **2012**, *42*, 1329.
[61] L. Mendive-Tapia, S. Preciado, J. Garcia, et al., *Nat. Commun.* **2015**, *6*, 7160.
[62] M. Todorovic, K. D. Schwab, J. Zeisler, C. Zhang, F. Benard, D. M. Perrin, *Angew. Chem. Int. Ed.* **2019**, *58*, 14120.
[63] X. Ma, J. Jia, R. Cao, X. Wang, H. Fei, *J. Am. Chem. Soc.* **2014**, *136*, 17734.
[64] O. Demeter, A. Kormos, C. Koehler, G. Mező, K. Németh, E. Kozma, L. B. Takács, E. A. Lemke, P. Kele, *Bioconjug. Chem.* **2017**, *28*, 1552.
[65] F. P. Verbeek, J. R. van der Vorst, Q. R. Tummers, et al., *Ann. Surg. Oncol.* **2014**, *21*, S528.
[66] S. Lee, X. Chen, *Mol. Imaging* **2009**, *8*, 87.
[67] J. Napp, M. A. Stammes, J. Claussen, H. A. J. M. Prevoo, C. F. M. Sier, F. J. M. Hoeben, M. S. Robillard, A. L. Vahrmeijer, T. Devling, A. B. Chan, L. F. de Geus-Oei, F. Alves, *Int. J. Cancer* **2018**, *142*, 2118.
[68] Y. Ye, B. Xu, G. V. Nikiforovich, S. Bloch, S. Achilefu, *Bioorg. Med. Chem. Lett.* **2011**, *21*, 2116.
[69] H. J. Cho, S. J. Lee, S. J. Park, C. H. Paik, S. M. Lee, S. Kim, Y. S. Lee, *J. Control. Release* **2016**, *237*, 177.
[70] J. Cao, R. Ge, M. Zhang, J. Xia, S. Han, W. Lu, Y. Liang, T. Zhang, Y. Sun, *Nanoscale* **2018**, *10*, 9021.
[71] H. J. Cho, S. J. Park, Y. S. Lee, S. Kim, *J. Control. Release* **2019**, *300*, 73.
[72] F. Reichart, O. V. Maltsev, T. G. Kapp, A. F. B. Räder, M. Weinmüller, U. K. Marelli, J. Notni, A. Wurzer, R. Beck, H. J. Wester, K. Steiger, S. di Maro, F. S. di Leva, L. Marinelli, M. Nieberler, U. Reuning, M. Schwaiger, H. Kessler, *J. Med. Chem.* **2019**, *62*, 2024.
[73] S. K. Shaw, W. Liu, C. F. A. Gomez Duran, et al., *Chem. Eur. J.* **2018**, *24*, 13821.

[74] Q. Li, W. Gu, K. Liu, N. Xiao, J. Zhang, L. Shao, L. Li, S. Zhang, P. Li, *RSC Adv.* **2016**, *6*, 74560.
[75] Y. Ye, W. Akers, B. Xu, S. Bloch, C. Odonkor, S. Achilefu, *Bioorg. Med. Chem. Lett.* **2012**, *22*, 5405.
[76] Y. Zheng, S. Ji, A. Czerwinski, F. Valenzuela, M. Pennington, S. Liu, *Bioconjug. Chem.* **2014**, *25*, 1925.
[77] F. Zhang, G. Niu, X. Lin, O. Jacobson, Y. Ma, H. S. Eden, Y. He, G. Lu, X. Chen, *Amino Acids* **2012**, *42*, 2343.
[78] Y. Raghuwanshi, H. Etayash, R. Soudy, I. Paiva, A. Lavasanifar, K. Kaur, *J. Med. Chem.* **2017**, *60*, 4893.
[79] R. Soudy, C. Chen, K. Kaur, *J. Med. Chem.* **2013**, *56*, 7564.
[80] N. D. Barth, R. Subiros-Funosas, L. Mendive-Tapia, et al., *Nat. Commun.* **2020**.
[81] C. Madhu, C. Voshavar, K. Rajasekhar, T. Govindaraju, *Org. Biomol. Chem.* **2017**, *15*, 3170.
[82] D. D. Rocha, V. R. Espejo, J. D. Rainier, J. J. La Clair, L. V. Costa-Lotufo, *Life Sci.* **2015**, *136*, 163.
[83] T. Soudah, S. Khawaled, R. I. Aqeilan, E. Yavin, *ACS Omega.* **2019**, *4*, 13954.
[84] A. H. Negussie, J. L. Miller, G. Reddy, S. K. Drake, B. J. Wood, M. R. Dreher, *J. Control. Release* **2010**, *143*, 265.
[85] H. J. M. Handgraaf, M. C. Boonstra, H. A. J. M. Prevoo, et al., *Oncotarget* **2017**, *8*, 21054.
[86] S. K. Shaw, C. L. Schreiber, F. M. Roland, P. M. Battles, S. P. Brennan, S. J. Padanilam, B. D. Smith, *Bioorg. Med. Chem.* **2018**, *26*, 2085.
[87] H. Shi, J. Liu, J. Geng, B. Z. Tang, B. Liu, *J. Am. Chem. Soc.* **2012**, *134*, 9569.
[88] D. Ding, J. Liang, H. Shi, R. T. K. Kwok, M. Gao, G. Feng, Y. Yuan, B. Z. Tang, B. Liu, *J. Mater. Chem. B* **2014**, *2*, 231.
[89] D. W. Hwang, N. Bahng, K. Ito, S. Ha, M. Y. Kim, E. Lee, H. Suga, D. S. Lee, *Cancer Lett.* **2017**, *385*, 144.
[90] S. Liu, Y. Zheng, D. Volpi, M. el-Kasti, D. Klotz, I. Tullis, A. Henricks, L. Campo, K. Myers, A. Laios, P. Thomas, T. Ng, S. Dhar, C. Becker, B. Vojnovic, A. A. Ahmed, *Cancer* **2015**, *121*, 202.
[91] J. Burggraaf, I. M. Kamerling, P. B. Gordon, et al., *Nat. Med.* **2015**, *21*, 955.
[92] I. A. Karpenko, R. Kreder, C. Valencia, P. Villa, C. Mendre, B. Mouillac, Y. Mély, M. Hibert, D. Bonnet, A. S. Klymchenko, *Chembiochem* **2014**, *15*, 359.
[93] M. Corbani, M. Trueba, S. Stoev, B. Murat, J. Mion, V´. Boulay, G. Guillon, M. Manning, *J. Med. Chem.* **2011**, *54*, 2864.
[94] N. Cui, M. Hu, R. A. Khalil, *Prog. Mol. Biol. Transl. Sci.* **2017**, *147*, 1.
[95] A. Alaseem, K. Alhazzani, P. Dondapati, S. Alobid, A. Bishayee, A. Rathinavelu, *Semin. Cancer Biol.* **2019**, *56*, 100.
[96] W. Wang, R. Shao, Q. Wu, S. Ke, J. McMurray, F. F. Lang Jr., C. Charnsangavej, J. G. Gelovani, C. Li, *Mol. Imaging Biol.* **2009**, *11*, 424.
[97] C. M. Lee, D. Jang, S. J. Cheong, M. H. Jeong, E. M. Kim, D. W. Kim, S. T. Lim, M. H. Sohn, H. J. Jeong, *Int. J. Cancer* **2012**, *131*, 1846.
[98] S. Shao, Z. Li, H. Cheng, S. Wang, N. G. Perkins, P. Sarkar, W. Wei, M. Xue, *J. Am. Chem. Soc.* **2018**, *140*, 13586.
[99] L. J. Wang, H. S. Li, Q. S. Wang, et al., *Contrast Media Mol. Imaging* **2018**, *2018*, 1.
[100] Z. Han, Z. Zhou, X. Shi, J. Wang, X. Wu, D. Sun, Y. Chen, H. Zhu, C. Magi-Galluzzi, Z. R. Lu, *Bioconjug. Chem.* **2015**, *26*, 830.
[101] C. A. Davies-Venn, B. Angermiller, N. Wilganowski, P. Ghosh, B. R. Harvey, G. Wu, S. Kwon, M. B. Aldrich, E. M. Sevick-Muraca, *Mol. Imaging Biol.* **2012**, *14*, 301.
[102] H. K. Jung, K. Wang, M. K. Jung, I. S. Kim, B. H. Lee, *PLoS One* **2014**, *9*, e100341.
[103] L. G. Milroy, S. Rizzo, A. Calderon, B. Ellinger, S. Erdmann, J. Mondry, P. Verveer, P. Bastiaens, H. Waldmann, L. Dehmelt, H. D. Arndt, *J. Am. Chem. Soc.* **2012**, *134*, 8480.
[104] R. Gerasimaite, J. Seikowski, J. Schimpfhauser, et al., *Org. Biomol. Chem.* **2020**, *18*, 2929.
[105] A. Fernandez, E. J. Thompson, J. W. Pollard, T. Kitamura, M. Vendrell, *Angew. Chem. Int. Ed.* **2019**, *58*, 16894.
[106] A. Fernandez, M. Vermeren, D. Humphries, R. Subiros-Funosas, N. Barth, L. Campana, A. MacKinnon, Y. Feng, M. Vendrell, *ACS Cent. Sci.* **2017**, *3*, 995.
[107] M. Vendrell, A. Samanta, S. W. Yun, Y. T. Chang, *Org. Biomol. Chem.* **2011**, *9*, 4760.
[108] A. Samanta, M. Vendrell, S. W. Yun, Z. Guan, Q. H. Xu, Y. T. Chang, *Chem. Asian J.* **2011**, *6*, 1353.
[109] A. Samanta, M. Vendrell, R. Das, Y. T. Chang, *Chem. Commun.* **2010**, *46*, 7406.
[110] S. Benson, A. Fernandez, N. D. Barth, F. de Moliner, M. H. Horrocks, C. S. Herrington, J. L. Abad, A. Delgado, L. Kelly, Z. Chang, Y. Feng, M. Nishiura, Y. Hori, K. Kikuchi, M. Vendrell, *Angew. Chem. Int. Ed.* **2019**, *58*, 6911.
[111] R. J. Mellanby, J. I. Scott, I. Mair, A. Fernandez, L. Saul, J. Arlt, M. Moral, M. Vendrell, *Chem. Sci.* **2018**, *9*, 7261.
[112] Z. Cheng, W. O. Valenca, G. G. Dias, et al., *Bioorg. Med. Chem.* **2019**, *27*, 3938.
[113] F. de Moliner, A. King, G. G. Dias, G. F. de Lima, C. A. de Simone, E. N. da Silva Júnior, M. Vendrell, *Front. Chem.* **2018**, *6*, 339.
[114] H. Lee, W. Akers, K. Bhushan, S. Bloch, G. Sudlow, R. Tang, S. Achilefu, *Bioconjug. Chem.* **2011**, *22*, 777.
[115] H. S. Choi, S. L. Gibbs, J. H. Lee, S. H. Kim, Y. Ashitate, F. Liu, H. Hyun, G. L. Park, Y. Xie, S. Bae, M. Henary, J. V. Frangioni, *Nat. Biotechnol.* **2013**, *31*, 148.
[116] J. Sun, Z.-G. Teng, Y. Tian, J. D. Wang, Y. Guo, D. H. Kim, A. C. Larson, G. M. Lu, *Int. J. Clin. Exp. Med.* **2014**, *7*, 4747.
[117] Y. Cheng, C. Sun, X. Ou, B. Liu, X. Lou, F. Xia, *Chem. Sci.* **2017**, *8*, 4571.
[118] F. Thoreau, L. Vanwonterghem, M. Henry, J. L. Coll, D. Boturyn, *Org. Biomol. Chem.* **2018**, *16*, 4101.
[119] N. D. Barth, J. A. Marwick, M. Vendrell, A. G. Rossi, I. Dransfield, *Front. Immunol.* **2017**, *8*, 1708.
[120] C. Kao, R. Chandna, A. Ghode, C. Dsouza, M. Chen, A. Larsson, S. H. Lim, M. Wang, Z. Cao, Y. Zhu, G. S. Anand, R. Ge, *EBioMedicine* **2018**, *33*, 22.
[121] T. M. Williams, R. Sable, S. Singh, M. G. H. Vicente, S. D. Jois, *Chem. Biol. Drug Des.* **2018**, *91*, 605.
[122] K. Kelly, H. Alencar, M. Funovics, U. Mahmood, R. Weissleder, *Cancer Res.* **2004**, *64*, 6247.
[123] D. Wu, H. C. Daly, M. Grossi, E. Conroy, B. Li, W. M. Gallagher, R. Elmes, D. F. O'Shea, *Chem. Sci.* **2019**, *10*, 6944.
[124] S. J. Park, H. C. Yeo, N. Y. Kang, H. Kim, J. Lin, H. H. Ha, M. Vendrell, J. S. Lee, Y. Chandran, D. Y. Lee, S. W. Yun, Y. T. Chang, *Stem Cell Res.* **2014**, *12*, 730.
[125] M. Vendrell, S. J. Park, Y. Chandran, C. L. K. Lee, H. H. Ha, N. Y. Kang, S. W. Yun, Y. T. Chang, *Stem Cell Res.* **2012**, *9*, 185.
[126] T. Kitamura, J. W. Pollard, M. Vendrell, *Trends Biotechnol.* **2017**, *35*, 5.
[127] A. R. Akram, N. Avlonitis, E. Scholefield, M. Vendrell, N. McDonald, T. Aslam, T. H. Craven, C. Gray, D. S. Collie, A. J. Fisher, P. A. Corris, T. Walsh, C. Haslett, M. Bradley, K. Dhaliwal, *Sci. Rep.* **2019**, *9*, 8422.
[128] A. Fernandez, M. Vendrell, *Biochemistry* **2018**, *57*, 175.
[129] Z. Yi, Z. Luo, N. D. Barth, et al., *Adv. Mater.* **2019**, *31*, e1901851.

AUTHOR BIOGRAPHIES

LORENA MENDIVE-TAPIA studied chemistry at the University of Barcelona, Spain (BSc., MSc), and received her PhD degree in 2017 from the same university. She was awarded the Enrique Fuentes Quintana Award in 2018 for her work on the postsynthetic modification of peptides using chemoselective C-arylation methodologies. Currently she is a postdoctoral fellow at the University of Edinburgh, Scotland, and her research is focused on the development of new fluorescent probes for bioimaging.

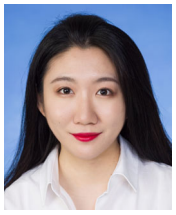

JINLING WANG studied bioengineering at Tianjin University, China (BSc), and she has recently graduated in chemistry at the University of Edinburgh, Scotland (BSc, MChem). Her MChem project was based on the development of new fluorogenic amino acids for the synthesis of fluorescent peptides for bioimaging.

MARC VENDRELL graduated in chemistry in 2007 before joining the Singapore Bioimaging Consortium to work with Young-Tae Chang in fluorophores for bioimaging. In 2012, he started his independent career at the University of Edinburgh, Scotland, where his group develops activatable fluorophores for imaging cancer and inflammation. He has recently been awarded an ERC Consolidator Grant (2017), the Marcial Moreno Lectureship (2018) and a SRUK Emerging Talent Award (2019). Beginning in 2020, he now holds a Personal Chair in Translational Chemistry and Biomedical Imaging.

How to cite this article: Mendive-Tapia L, Wang J, Vendrell M. Fluorescent cyclic peptides for cell imaging. *Peptide Science*. 2020;e24181. https://doi.org/10.1002/pep2.24181